J|A|C|S
ARTICLES
Published on Web 10/19/2002

Membrane Affinity of the Amphiphilic Marinobactin Siderophores

Guofeng Xu,[†] Jennifer S. Martinez,[‡] John T. Groves,*[,†] and Alison Butler*[,‡]

Contribution from the Department of Chemistry, Princeton University, Princeton, New Jersey 08544, and Department of Chemistry and Biochemistry, University of California, Santa Barbara, California 93106

Received May 2, 2002

Abstract: Marinobactins are a class of newly discovered marine bacterial siderophores with a unique amphiphilic structure, suggesting that their functions relate to interactions with cell membranes. Here we use small and large unilamellar L-α-dimyristoylphosphatidylcholine vesicles (SUVs and LUVs) as model membranes to examine the thermodynamics and kinetics of the membrane binding of marinobactins, particularly marinobactin E (apo-M_E) and its iron(III) complex, Fe−M_E. Siderophore−membrane interactions are characterized by NMR line broadening, stopped-flow spectrophotometry, fluorescence quenching, and ultracentrifugation. It is determined that apo-M_E has a strong affinity for lipid membranes with molar fraction partition coefficients $K_x^{\text{apo-M}_E} = 6.3 \times 10^5$ for SUVs and 3.6×10^5 for LUVs. This membrane association is shown to cause only a 2-fold decrease in the rate of iron(III) binding by apo-M_E. However, upon the formation of the iron(III) complex Fe−M_E, the membrane affinity of the siderophore decreased substantially ($K_x^{\text{Fe-M}_E} = 1.3 \times 10^4$ for SUVs and 9.6×10^3 for LUVs). The kinetics of membrane binding and dissociation by Fe−M_E were also determined ($k_{on}^{\text{Fe-M}_E} = 1.01\ M^{-1}\ s^{-1}$; $k_{off}^{\text{Fe-M}_E} = 4.4 \times 10^{-3}\ s^{-1}$). The suite of marinobactins with different fatty acid chain lengths and degrees of chain unsaturation showed a range of membrane affinities (5.8×10^3 to $36\ M^{-1}$). The affinity that marinobactins exhibit for membranes and the changes observed upon iron binding could provide unique biological advantages in a receptor-assisted iron acquisition process in which loss of the iron-free siderophore by diffusion is limited by the strong association with the lipid phase.

Introduction

Iron is one of the earth's most abundant crustal elements. The use of this element in enzymes and cofactors is ubiquitous in nature, and with the possible exception of lactobacteria and *Borrelia burgdorferi*, all microorganisms require iron for growth.[1] However, the acquisition of iron is difficult in aqueous aerobic conditions under which Fe(III) is highly insoluble. This problem is further compounded in the surface seawater of the ocean where total iron levels are vanishingly small (0.02−1 nM) and greater than 99% of the dissolved iron is complexed by organic ligands.[2,3] This low level of iron has been shown to limit primary production by phytoplankton in regions of the ocean characterized by high levels of nitrate and low levels of chlorophyll (HNLC regions).[4−7] In addition to phytoplankton and other photosynthetic (autotrophic) microorganisms, heterotrophic bacteria are potentially critical to the biogeochemical cycling of iron in the ocean and are another class of microorganisms limited by low iron levels associated with HNLC regions.[8−11]

The acquisition of iron by heterotrophic bacteria is facilitated by the production and release of low-molecular-weight, high-affinity iron chelators to solubilize iron(III) and promote its uptake. The production of these siderophores is regulated by iron levels, with repression of siderophore production under high iron conditions. Also regulated by iron levels are high-affinity receptor proteins that recognize siderophore−iron(III) complexes and transport them into the bacterial cell. A wide range of structures have been determined for siderophores produced by terrestrial and enteric bacteria;[12,13] however, few siderophores have been structurally characterized from marine bacteria and marine microorganisms.[8,14−18]

* To whom correspondence should be addressed. (J.T.G.) E-mail: jtgroves@princeton.edu. (A.B) E-mail: butler@chem.ucsb.edu.
[†] Princeton University.
[‡] University of California.

(1) Posey, J. E.; Gherardini, F. C. *Science* **2000**, *288*, 1651−1653.
(2) Wu, J.; Luther, G. W., III. *Mar. Chem.* **1995**, *50*, 159−177.
(3) Rue, E.; Bruland, K. W. *Mar. Chem.* **1995**, *50*, 117−138.
(4) Boyd, P. W.; et al. *Nature* **2000**, *407*, 695−702.
(5) Behrenfeld, M. J.; Bale, A. J.; Kolber, Z. S.; Aiken, J.; Falkowski, P. G. *Nature* **1996**, *383*, 508−511.
(6) Coale, K. H.; et al. *Nature* **1996**, *383*, 495−501.
(7) Hutchins, D. A.; Bruland, K. W. *Nature* **1998**, *393*, 561−564.
(8) Granger, J.; Price, N. M. *Limnol. Oceanogr.* **1999**, *44*, 541−555.
(9) Tortell, P. D.; Maldonado, M. T.; Granger, J.; Price, N. M. *FEMS Microbiol. Ecol.* **1999**, *29*, 1−11.
(10) Pakulski, J. D.; et al. *Nature* **1996**, *383*, 133−134.
(11) Tortell, P. D.; Maldonado, M. T.; Price, N. M. *Nature* **1996**, *383*, 330−332.
(12) Winkelmann, G. H. *Handbook of microbial iron chelates*; CRC Press: Boca Raton, FL, 1991.
(13) Albrecht-Gary, A. M.; Crumbliss, A. L. *Metal Ions in Biological Systems*; 1998; Vol. 35, pp 239−327.
(14) Haygood, M. G.; Holt, P. D.; Butler, A. *Limnol. Oceanogr.* **1993**, *38*, 1091−1097.
(15) Reid, R. T.; Live, D. H.; Faulkner, D. J.; Butler, A. *Nature* **1993**, *366*, 455−458.
(16) Butler, A. *Science* **1998**, *281*, 207−210.

10.1021/ja026768w CCC: $22.00

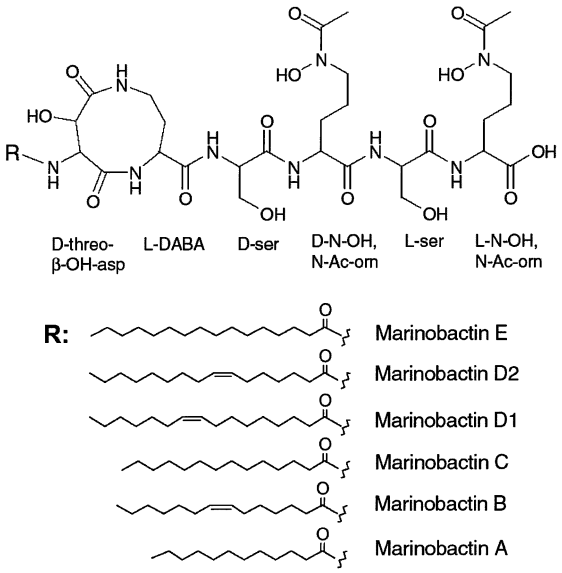

Figure 1. Structures of the amphiphilic marinobactins produced by the *Marinobacter* sp. strain DS40M6. Reprinted with permission from ref 17. Copyright 2000 American Association for the Advancement of Science.

One class of marine siderophores, the marinobactins and aquachelins, are unusual amphiphilic peptides (Figure 1). These two families were isolated from distinct genera of marine bacteria (*Halomonas aquamarina* and a *Marinobacter* species), yet each produces strikingly similar siderophores[17] containing a unique peptidic headgroup that coordinates iron(III) and one of a series of fatty acid appendages. These lipopeptides have surfactant properties and form micelles at low critical micelle concentrations (CMCs).[17] Bacterial lipopeptides[19] facilitate growth on hydrocarbons, have biocide activity toward Gram-positive bacteria and eucaryotic organisms, and condition surfaces to enable bacterial adherence and biofilm production.[20] The partitioning of such biosurfactants or amphiphilic polymers to microbial cell surfaces has been suggested as a means to change their cell surface hydrophobicity.[20] Whereas many lipopeptides of bacterial origin are known, few siderophores in nature are lipophilic.[12,13,21−25] It is therefore of interest to understand the interactions of the marinobactins and aquachelins with cell membranes and other lipid phases and to elucidate the molecular mechanisms involved in iron sequestration mediated by these amphiphilic siderophores. This understanding is also of general interest toward creating and utilizing functional biomaterials or bioactive surfaces. Toward this end we have investigated the interaction of the marinobactins with a model cell membrane, by studying the thermodynamics and kinetics of membrane partitioning as well as iron chelation of the siderophores in the presence of unilamellar phospholipid vesicles.

Experimental Section

Materials. L-α-Dimyristoylphosphatidylcholine (DMPC; 99+%), DMPC with deuterated *N*-methyl groups (DMPC-d_9), and 1,2-dimyristoyl-*sn*-glycero-3-phosphate (DMPi) were obtained from Avanti Polar Lipids, Inc. Ferric ammonium citrate (FAC) and potassium chloride were purchased from Aldrich. Lipidated pyrene (P-58) was purchased from Molecular Probes. Marinobactins and aerobactin were isolated as previously described.[14,17,30]

Preparation of Vesicles. Unilamellar vesicles were prepared by either sonication for small vesicles or membrane extrusion for large vesicles as previously described.[26,27] Briefly, thin films of DMPC were deposited on the side walls of 5 mL test tubes by evaporation of the DMPC chloroform solution under a stream of argon gas. The films were further dried under vacuum overnight. To prepare small unilamellar vesicles (SUVs), the lipid films were incubated and hydrated in buffer at room temperature for 30 min, and then the mixture was sonicated with a probe tip sonicator for 15 min until a translucent, blue suspension was formed. To prepare large unilamellar vesicles (LUVs), the lipid films were similarly incubated and hydrated, and then subjected to a few freeze−thaw cycles by alternately dipping the test tube in liquid nitrogen and warm water. The suspension was then extruded through a polycarbonate filter with an average pore size of 200 nm at 30 °C 20 times to yield a translucent LUV suspension. Dynamic light scattering, transmission electron microscopy, and NMR measurements were employed to establish the vesicular size. The SUVs had an average diameter of 30−40 nm, and the LUVs had an average diameter of 180 nm.

Stopped-Flow Spectroscopy. The kinetics of siderophore−iron(III) chelation in the presence of vesicles was studied by stopped-flow spectrophotometry (Hi-Tech SF-61 DX2). One mixing syringe was filled with 1 mM ferric ammonium citrate solution prepared in a Tris buffer (60 mM Tris, 0.1 M KCl, pH 8.0). The other mixing syringe was filled with 40 μM apo-M_E in Tris buffer preincubated for 30 min with varying amounts of SUVs. The concentration of the SUVs ranged from 0 to 20 mM. For each experiment, 200 μL was withdrawn from each syringe and mixed rapidly. The visible absorption of the mixture was monitored at 430 nm for the formation of the siderophore−iron(III) complex. Similar mixtures containing ferric ammonium citrate and vesicles without apo-M_E were used as the background. At each vesicle concentration, six mixing runs were performed and the spectral traces were averaged. The rates of complex formation were calculated from the initial slope of the averaged spectral traces between 0.5 and 2 s.

NMR Spectroscopy. Proton NMR experiments to study the partition of Fe−M_E into SUV membranes were carried out using a Varian INOVA 500 MHz instrument with the probe maintained at 25 °C. DMPC SUV suspensions were prepared in Tris buffer (60 mM, 0.1 M KCl, pH 8.0) using D_2O as the solvent. The choline *N*-methyl groups of DMPC were used as the indicator to study the line-broadening effect by the siderophore−iron(III) complexes. Two well-resolved ^{1}H resonances were observed at 25 °C for the *N*-methyl groups, corresponding to the outer membrane leaflet at δ 3.286 and the inner membrane leaflet appearing at δ 3.238. In a typical experiment, the spectrum of the blank vesicle suspension was first recorded over 16 pulses. Fe−M_E was introduced into the NMR tube for a final concentration of 40 μM. The sample was incubated for 60 min before the final spectrum was taken again with 16 pulses. The line widths at the half-heights of the *N*-methyl resonances were obtained by fitting a Gaussian line profile to the corresponding peaks in the spectral region between δ 3.160 and δ 3.360.

(17) Martinez, J. S.; Zhang, G. P.; Holt, P. D.; Jung, H.-T.; Carrano, C. J.; Haygood, M. G.; Butler, A. *Science* **2000**, *287*, 1245−1247.
(18) Wilhelm, S. W.; Trick, C. G. *Limnol. Oceanogr.* **1994**, *39*, 1974−1984.
(19) Ahimou, F.; Jacques, P.; Deleu, M. *Enzyme Microb. Technol.* **2000**, *27*, 749−754.
(20) Neu, T. R. *Microbiol. Rev.* **1996**, *60*, 151−166.
(21) Gobin, J.; Moore, C. H.; Reeve, J. R.; Wong, D. K.; Gibson, B. W.; Horwitz, M. A. *Proc. Natl. Acad. Sci. U.S.A.* **1995**, *92*, 5189−5193.
(22) Gobin, J.; Horowitz, M. A. *J. Exp. Med.* **1996**, *183*, 1527−1532.
(23) Stephan, H.; Freund, S.; Beck, W.; Jung, G.; Meyer, J. M.; Winkelmann, G. *BioMetals* **1993**, *6*, 93−100.
(24) Risse, D.; Beiderbeck, H.; Taraz, K.; Budzikiewicz, H.; Gustine, D. *Z. Naturforsch., C* **1998**, *53*, 295−304.
(25) Okujo, N.; Sakakibara, Y.; Yoshida, T.; Yamamoto, S. *Biometals* **1994**, *7*, 170−176.
(26) (a) Lahiri, J.; Fate, G. D.; Ungashe, S. B.; Groves, J. T. *J. Am. Chem. Soc.* **1996**, *118*, 2347−2358. (b) Ungashe, S. B.; Groves, J. T. Porphyrins and Metalloporphyrins in Synthetic Bilayer Membranes. In *Advances in Inorganic Biochemistry*; Marzilli, L. G., Ed.; Academic Press: New York, 1993; Vol. 9, pp 318−351.
(27) Mayer, L. D.; Hope, M. J.; Cullis, P. R. *Biochim. Biophys. Acta* **1986**, *858*, 161−168.

Scheme 1. A Schematic Presentation of the Membrane Partition of apo-M_E and Fe−M_E and the Iron(III) Acquisition by apo-M_E from FAC

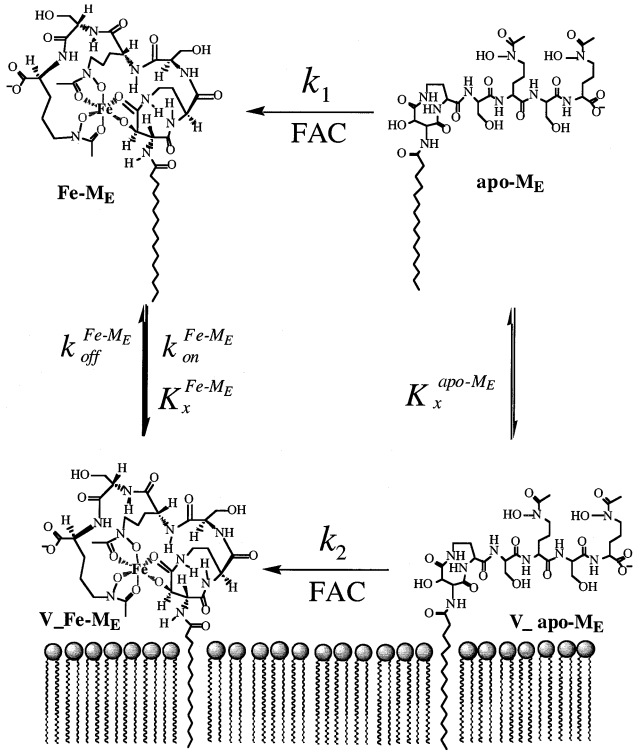

Fluorescence Quenching Experiments. Fluorescence measurements of pyrene−PC were made on a Varian Eclipse spectrofluorimeter. Excitation and emission wavelengths were 351 and 400 nm, respectively. SUVs (see Preparation of Vesicles) containing 3 mM DMPC and 0.2 μM pyrene−PC or 3 mM DMPi and 0.15 μM pyrene−PC were prepared by sonication in 10 mM Tris−HCl, 0.1 M KCl (pH 8.0). Siderophores (apo-M_E or Fe−M_E) or FAC was added at a 15 or 40 μM concentration, respectively. Apo-M_E was added either prior to, as a 4 h equilibration with vesicles, or following FAC addition. Pyrene−PC at the surface of the vesicle acted as a fluorescence donor and the Fe(III)−M_E as acceptor. Quenching of pyrene emission was taken as an indication of siderophore association with the membrane. All experiments were completed at 27 °C.

Centrifugation Experiments. The partition coefficient of apo-marinobactins and Fe(III)−marinobactins between the membrane and the water phases of DMPC LUVs was measured by HPLC. Varying concentrations of extruded vesicles were incubated with 16.2 μM apo-M_E or 20.5 μM Fe−M_E in acid-washed polyallomer centrifuge tubes in the dark at 27 °C with gentle shaking. After a 2.5 h equilibration, the siderophore/vesicle mixture was centrifuged at 200000*g* for 3 h. The supernatant was removed and assayed by HPLC for siderophore concentration using a C4 reversed-phase column (Vydac, 4.6 mm i.d. × 250 mm length) with a linear gradient of 0−100% B over 37 min [A = 99.95% *d*-H_2O and 0.05% trifluoroacetic acid (TFA); B = 19.95% *d*-H_2O, 0.05% TFA, and 80% acetonitrile]. The absorbance of the eluent was monitored at 215 nm. The concentration of siderophore remaining in the supernatant was determined by comparing the area of the chromatographic peak to a standard curve for each siderophore. Similar experiments were completed with the physiological mixture of marinobactins.

Results and Interpretation

Phospholipid Partition Coefficient and Iron(III) Binding Kinetics of Apo-M_E in SUV Membranes. Scheme 1 depicts the pathways of iron(III) chelation by apo-M_E in the presence of lipid vesicles. The rates of chelation were measured by stopped-flow spectroscopy with variable concentrations of lipid. With a large excess of iron(III), the initial formation rate of Fe−M_E can be expressed as shown in eq 1.[28]

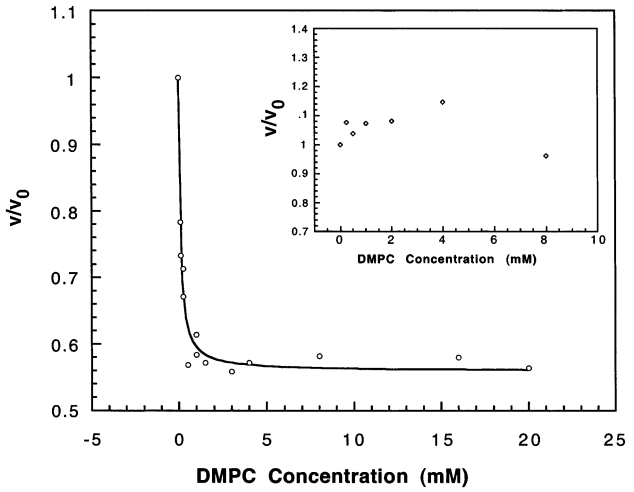

Figure 2. Relative iron(III) chelation rate by apo-M_E as a function of DMPC concentration at 0.5 mM ferric ammonium citrate and 20 μM apo-M_E (final concentration after mixing) determined by stopped-flow spectroscopy at pH 8. The solid line is the curve-fitting result, using eq 2. Inset: Change of the relative initial rate of iron binding by aerobactin as a function of DMPC concentration.

$$v = \frac{\mathrm{d[Fe{-}M_E]}}{\mathrm{d}t} = k_1[\text{apo-M}_E]_w + k_2[\text{apo-M}_E]_l \qquad (1)$$

The rate of formation of Fe−M_E is assumed to contain contributions from the siderophore in both the aqueous (k_1) and lipid (k_2) phases. Considering the mass balance, one can obtain the relationship shown in eq 2.[29]

$$\frac{v}{v_0} = \frac{1 + (k_2/k_1)K^*_{\text{apo-M}_E}[\mathrm{L}]}{1 + K^*_{\text{apo-M}_E}[\mathrm{L}]} \qquad (2)$$

Equation 2 predicts a hyperbolic relationship between the relative initial chelation rate (v/v_0) and the lipid concentration ([L]). Figure 2 shows the relative chelation rate for a given amount of apo-M_E at different lipid (DMPC) concentrations, as monitored by observing the visible absorption of Fe−M_E at 430 nm. In accord with eq 2, the observed chelation rate decreased rapidly as the lipid concentration increased from 0 to about 1 mM, and then approached a constant value at higher lipid-phase concentrations. The decrease of the chelation rate indicates that the vesicle-bound apo-M_E chelates iron(III) about 2 times more slowly than free apo-M_E.

(28) $[\text{apo-M}_E]_w$ is the molar concentration of apo-M_E in the water phase as calculated from the total volume of the vesicular suspension, $[\text{apo-M}_E]_l$ is the molar concentration of apo-M_E in the lipid phase, and $[\text{apo-M}_E]_0$ is the molar concentration of the total apo-M_E in the vesicular suspension.

(29) $K_x^{\text{apo-M}_E} = x_l^{\text{apo-M}_E}/x_w^{\text{apo-M}_E} = ([\text{apo-M}_E]_l/[\mathrm{L}])/([\text{apo-M}_E]_w/[\mathrm{H_2O}]) = K^*_{\text{apo-M}_E}[\mathrm{H_2O}]$, where $K_x^{\text{apo-M}_E}$ is the partition coefficient of apo-M_E based on the molar fraction, $K^*_{\text{apo-M}_E}$ is an alternatively defined partition coefficient of apo-M_E (M^{-1}), $x_l^{\text{apo-M}_E}$ is the mole ratio of membrane-bound apo-M_E to lipid, $x_l^{\text{apo-M}_E}$ is the mole ratio of free apo-M_E to water, [L] is the molar concentration of the lipid, and $[\mathrm{H_2O}]$ is the molar concentration of water. For the derivation of eq 2, see the Supporting Information.

(30) Harris, W. R.; Carrano, C. J.; Raymond, K. N. *J. Am. Chem. Soc.* **1979**, *101*, 2722−2727.

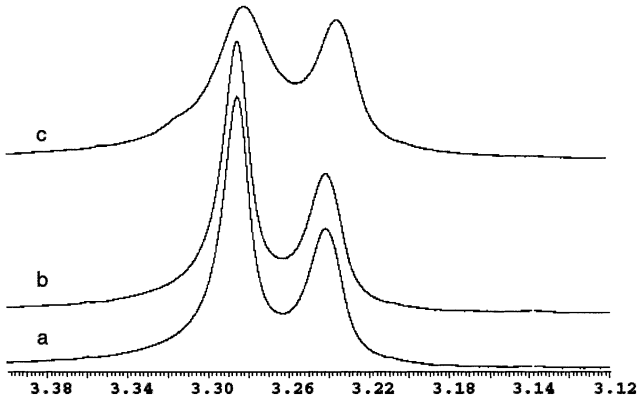

Figure 3. NMR line-broadening effect on the resonance peaks of DMPC vesicle choline methyl groups, due to the insertion of Fe−M_E into the vesicle membrane: (a) DMPC vesicles; (b) DMPC vesicles with 40 μM aerobactin; (c) DMPC vesicles with 40 μM Fe−M_E. The outer membrane leaflet is observed at δ 3.286 and the inner membrane leaflet at δ 3.238.

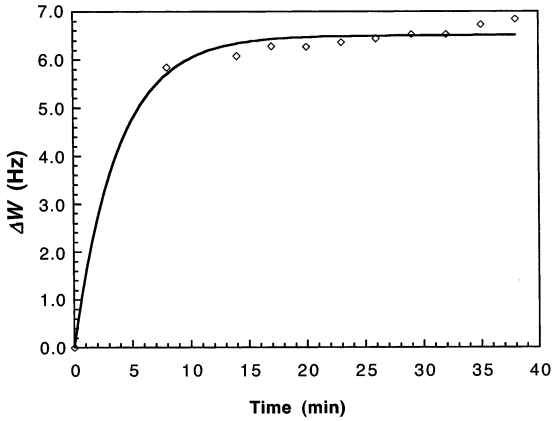

Figure 4. Time-dependent line broadening of the outer leaflet *N*-methyl ^{1}H resonance of 10 mM protio-DMPC vesicles upon mixing with 10 mM DMPC-d_9 preincubated with 40 μM Fe−M_E.

At lipid concentrations greater that 1 mM, nearly all of the apo-M_E molecules are associated with the vesicles. Control experiments with a nonamphiphilic and water-soluble siderophore, aerobactin[14,30] (Figure 2, inset), showed no effect of the vesicle phase. Fitting the rate data for iron binding by apo-M_E (Figure 2) with eq 2 yields a partition coefficient of 1.1×10^4 M^{-1} ($K^*_{\text{apo-}M_E}$) or 6.3×10^5 ($K_x^{\text{apo-}M_E}$). The curve fitting also yielded the ratio of the pseudo-first-order chelation rate constant for the vesicle-bound apo-M_E and the free apo-M_E (k_2/k_1 = 0.56). Thus, a dissociative process involving iron acquisition from FAC by *free* apo-M_E (k_1 in Scheme 1) is insignificant in comparison to the membrane-bound process k_2 in the presence of 1 mM or greater lipid-phase concentration.

Partitioning of Fe−M_E into SUV Membranes Probed by NMR. The partitioning of high-spin Fe(III)−M_E into the lipid membrane of SUVs was probed by NMR line-broadening techniques. The two leaflets of the SUV bilayer membrane are highly asymmetric, and the corresponding choline *N*-methyl groups are spectroscopically distinguishable by proton NMR.[31,32]

As shown in Figure 3, the addition of Fe−M_E to a DMPC vesicle suspension caused a dramatic broadening of the [^{1}H]-choline resonance corresponding to the outer membrane leaflet. By contrast little change in the line width was observed upon addition of aerobactin−iron(III) complex. Thus, the results indicate that Fe−M_E also partitions into the lipid membranes.[33]

Kinetics of Membrane Binding and Dissociation of Fe−M_E As Probed by NMR. To investigate whether the partitioning of Fe−M_E into lipid membranes is reversible, we designed the following *mixed-vesicle* experiments. Fe−M_E was incubated with a suspension of SUVs composed of choline *N*-methyl-deuterated DMPC-d_9. The mixture was added to a suspension of SUVs composed of *proteo*-DMPC at the same lipid concentration but without the iron(III)−siderophore complex. The NMR ^{1}H resonance of the choline *N*-methyl of proteo-DMPC was monitored and used as an indicator of the redistribution of the Fe−M_E molecules.[34,35] Figure 4 shows the change of the line width at half-maximum (LWHM) of the *N*-methyl resonances of the proteo-DMPC vesicles upon mixing the two populations of vesicles (DMPC and DMPC-d_9 containing Fe−M_E). As can be seen, the line width of the outer membrane leaflet broadened significantly within 5 min, indicating a fast membrane partitioning equilibrium.

A quantitative analysis of the line-broadening effect shown in Figure 4 provided a measure of the rate of Fe−M_E dissociation from the lipid membrane. Consider the following two equilibria before and after an equal volume mixing of the two vesicle suspensions with the same lipid concentrations (V = DMPC vesicles; V-d_9 = DMPC-d_9 vesicles):[36]

$$\text{V-}d_9\text{–Fe–M}_E \underset{k_{\text{on}}^{\text{Fe–M}_E}}{\overset{k_{\text{off}}^{\text{Fe–M}_E}}{\rightleftharpoons}} \text{Fe–M}_E \underset{k_{\text{off}}^{\text{Fe–M}_E}}{\overset{k_{\text{on}}^{\text{Fe–M}_E}}{\rightleftharpoons}} \text{V–Fe–M}_E$$

Before mixing, Fe−M_E is at equilibrium between the DMPC-d_9 vesicles and the buffer. Upon mixing, the Fe−M_E concentration in the buffer decreases by half, while the Fe−M_E concentration in the DMPC-d_9 vesicles initially remains the same. To reestablish equilibrium, Fe−M_E in the buffer will bind rapidly to the protio-DMPC and the Fe−M_E in the DMPC-d_9 vesicles will enter the buffer. However, because the overall Fe−M_E concentration in vesicles (DMPC and DMPC-d_9 combined) is also reduced to half upon mixing, the overall partition equilibrium between the buffer and the vesicles will be maintained. A net flux of the Fe−M_E molecules from DMPC-d_9 vesicles to DMPC vesicles occurs at the rate of the Fe−M_E leaving the DMPC vesicles. Assuming that the repartitioning is a first-order (dissociative) process, the above analysis can be expressed in the following equation (see the Supporting Information for the derivation):

$$x = 0.5x^{\text{de}}[1 - \exp(-k_{\text{off}}^{\text{Fe–M}_E}t)] \qquad (3)$$

(31) Sheetz, M. P.; Chan, S. I. *Biochmeistry* **1972**, *11*, 4573-4581.
(32) Gunther, H. *NMR Spectroscopy*; John Wiley & Sons: New York, 1995.
(33) The outer membranes of Gram-negative bacteria are negatively charged as a result of the predominance of lipopolysaccharide (LPS). Experiments were completed on vesicles made of LPS from *E. coli*. Results from these experiments suggest that Fe−M_E rapidly associates with these vesicles (results not shown) and behaves similarly to those experiments with DMPC, which are characterized by zwitterionic headgroups.
(34) The underlying assumption of the experiments is that no vesicle fusion or lipid exchange between vesicles occurs during the experiments. As these two processes are usually much slower than the partition equilibria, their effects of skewing the experimental results can be ignored.
(35) Rosoff, M., Ed. *Vesicles*; Marcel Dekker: New York, 1996; Vol. 62.
(36) The process assumes a mixing of equal volumes to simplify the derivation; however, the volume ratio of the two vesicle suspensions does not affect the conclusions as long as they have the same concentration.

where x^{de} is the mole ratio of the Fe−M_E in DMPC-d_9 vesicles at equilibrium before mixing and x is the mole ratio of the Fe−M_E in protio-DMPC vesicles during the redistribution.

Assuming the NMR line broadening is proportional to the mole ratio of siderophore to DMPC, the time-dependent line width change ($\Delta W(t)$) can be expressed as follows:

$$\Delta W(t) = (\text{const})0.5x^{de}[1 - \exp(-k_{off}^{Fe-M_E}t)] = (\Delta W)[1 - \exp(-k_{off}^{Fe-M_E}t)] \quad (4)$$

where ΔW stands for the line width change when the partition equilibrium is reached. Thus, the rate of the Fe−M_E dissociation from the vesicles can be obtained by measuring the rate of the line broadening in the mixed-vesicle experiments. Fitting the data in Figure 4 with eq 4 yielded $k_{off}^{Fe-M_E} = 4.4 \times 10^{-3}$ s^{-1}. This value is the lower limit of $k_{off}^{Fe-M_E}$ since the data did not capture the earlier moments immediately after the mixing due to the "dead time" of handling the samples in the NMR experiments.

Membrane Partition Coefficient of Fe−M_E in SUVs Determined by NMR. The NMR line-broadening effect also allowed us to measure the lipid partition coefficient of Fe−M_E. When the molar ratio of Fe−M_E to lipid was very low (e.g., $x_l^{Fe-M_E} < 1\%$), its effect on the NMR line width was linear with respect to this ratio. Neglecting the effect of free Fe−M_E in solution, the change of the LWHM for the resonances of the choline *N*-methyl groups in the outer membrane can be expressed as follows:

$$\Delta W = W - W_0 = Ax_l^{Fe-M_E} \quad (5)$$

where W_0 and W are the LWHM of the *N*-methyl ^{1}H resonance of the outer membrane DMPC in the absence and presence of Fe−M_E, respectively, $x_l^{Fe-M_E}$ is the mole ratio of membrane-bound Fe−M_E to lipid, and A is a constant. Consideration of the mass balance and the partition equilibrium affords the following relationship:[37]

$$\frac{1}{\Delta W} = \frac{1}{A[Fe-M_E]_0}[L] + \frac{1}{A[Fe-M_E]_0}\frac{1}{K^*_{Fe-M_E}} \quad (6)$$

This equation predicts that, for a given amount of Fe−M_E added into the vesicle suspension, the reciprocal of the observed line width change ($1/\Delta W$) is a linear function of the lipid concentration ([L]). The lipid partition coefficient can be calculated from the ratio of the slope to the intercept. Figure 5 shows the results of the experiments in which a fixed amount of Fe−M_E was introduced to a DMPC SUV suspension at different concentrations. A linear plot was obtained using eq 6, and the lipid partition coefficient of Fe−M_E was determined to be 2.32×10^2 M^{-1} ($K^*_{Fe-M_E}$) or 1.3×10^4 ($K_x^{Fe-M_E}$), about *50 times smaller* than that of apo-M_E (6.3×10^5). Thus, binding iron significantly *decreases* the membrane affinity of marinobactin. From the partition coefficient and the rate of Fe−M_E dissociation from vesicles, the rate of Fe−M_E binding to vesicles can also be determined ($k_{on}^{Fe-M_E} = 1.01$ M^{-1} s^{-1}).

(37) $K_x^{Fe-M_E} = x_l^{Fe-M_E}/x_w^{Fe-M_E} = ([Fe\text{-}M_E]_l/[L])/([Fe\text{-}M_E]_w/[H_2O]) = K^*_{Fe-M_E}[H_2O]\,[Fe\text{-}M_E]_0 = [Fe\text{-}M_E]_w + [Fe\text{-}M_E]_l$, where all the variables and coefficients are defined similarly to those for apo-M_E. For the derivation of eq 6, see the Supporting Information.

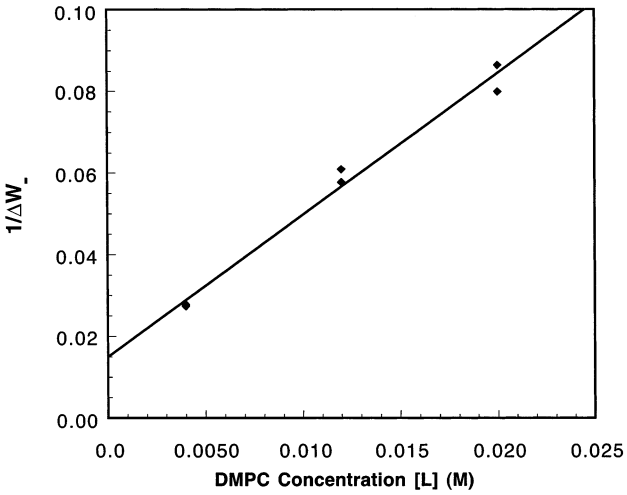

Figure 5. $1/\Delta W$ vs DMPC concentration ([L]) to determine the partition coefficient of Fe−M_E between vesicle and buffer. The solid line is the curve-fitting result by eq i (Supporting Information). The fitting yields the slope to be 3.48 M^{-1} and the intercept to be 1.50×10^{-2}. According to eq 6, the partition coefficient is then obtained as $K^*_{Fe-M_E}$ = slope/intercept = 2.32×10^2 M^{-1} or $K_x^{Fe-ME} = 1.29 \times 10^4$.

Interaction of Apo-M_E and Fe−M_E with SUVs Probed by Fluorescence Quenching. The interaction of Fe−M_E with vesicles was studied by fluorescence quenching of vesicle-bound pyrene by Fe−M_E, using vesicles composed of the zwitterionic lipid DMPC or the anionic lipid DMPi. Addition of 15 μM Fe−M_E rapidly quenched the vesicle-bound pyrene emission, indicating that Fe−M_E associates quickly with both DMPC and DMPi vesicles (Figure 6a,d). On the other hand, addition of 40 μM FAC quenched the pyrene emission in both DMPC and DMPi vesicles to a much lesser extent (see Figure 6c,e for 0−5 min) than that seen for 15 μM Fe−M_E. Subsequent addition of 15 μM apo-M_E to the equilibrated solution of pyrene vesicles and 40 μM FAC induced a slower rate of quenching, as a result of rapid association of apo-M_E with the vesicles and therefore slow Fe(III) coordination (Figure 6c,e after 5 min). This slower rate of Fe(III) coordination was also observed in stopped-flow results as described above. Furthermore, pyrene-bound DMPC vesicles preequilibrated with apo-M_E also showed a similar slow rate of pyrene quenching upon subsequent addition of FAC. The similarity in the fluorescence quenching results of the DMPC and DMPi vesicles, which differ in headgroup charge, suggests that the association of the marinobactins with vesicles is a result of partitioning the hydrophobic tails into the membrane of the vesicles and not an electrostatic interaction of the headgroup with the vesicles.

Partitioning of Apo-M_E and Fe−M_E into LUV Membranes As Determined by Ultracentrifugation and HPLC. Membrane partitioning of apo-M_E and Fe−M_E was examined in LUVs which contain well-packed planar surfaces[38,39] and relate in size to bacterial cells.[40,41] When a fixed concentration of apo-M_E or Fe−M_E was mixed with varying concentrations of DMPC vesicles, the ratio of siderophore remaining in solution (D_W) to the initial siderophore concentration (D_T) was found to be

(38) Jackson, M. L.; Schmidt, D.; Lichtenberg, D.; Litman, B. J.; Albert, A. D. *Biochemistry* **1982**, *21*, 4576−4582.
(39) Nordlund, J. R.; Schmidt, C. F.; Dicken, S. N.; Thompson, T. E. *Biochemistry* **1981**, *20*, 3237−3241.
(40) Azam, F.; Hodson, R. E. *Limnol. Oceanogr.* **1977**, *22*, 492−501.
(41) Campbell, L.; Nolla, H. A.; Vaulot, D. *Limnol. Oceanogr.* **1994**, *39*, 954−961.

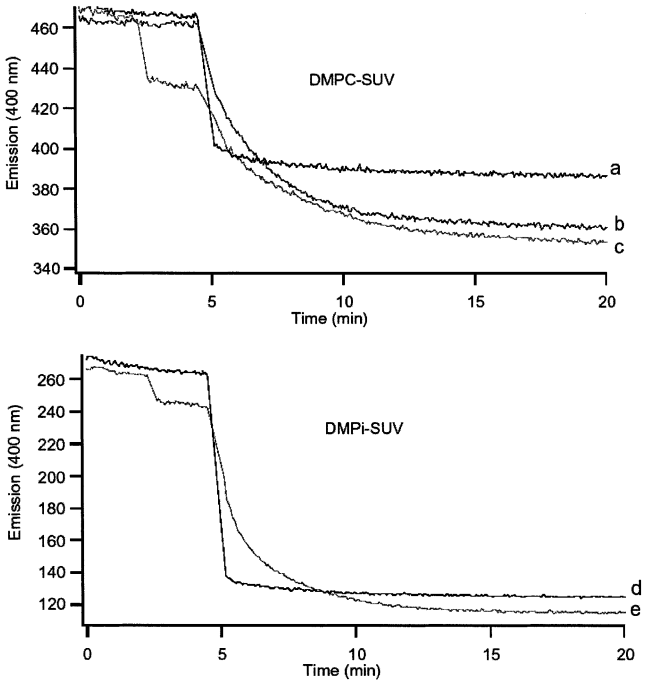

Figure 6. Fluorescence emission of pyrene−SUVs composed of DMPC or DMPi as a function of time. Small unilamellar vesicles contained 3 mM DMPC/0.2 μM pyrene−PC (A, top) or DMPi/0.15 μM pyrene−PC (B, bottom) in 10 mM Tris−HCl, 0.1 M KCl (pH 8.0). Excitation and emission wavelengths were 351 and 400 nm, respectively. (a, d) A 15 μM concentration of Fe−M_E was added to the vesicles at 5 min. (b) A 15 μM concentration of apo-M_E was preequilibrated with the vesicles for 4 h prior to addition of 40 μM FAC at 5 min. (c, e) A 40 μM concentration of FAC was added to the vesicles at 2.5 min followed by addition of 15 μM apo-M_E at 5 min.

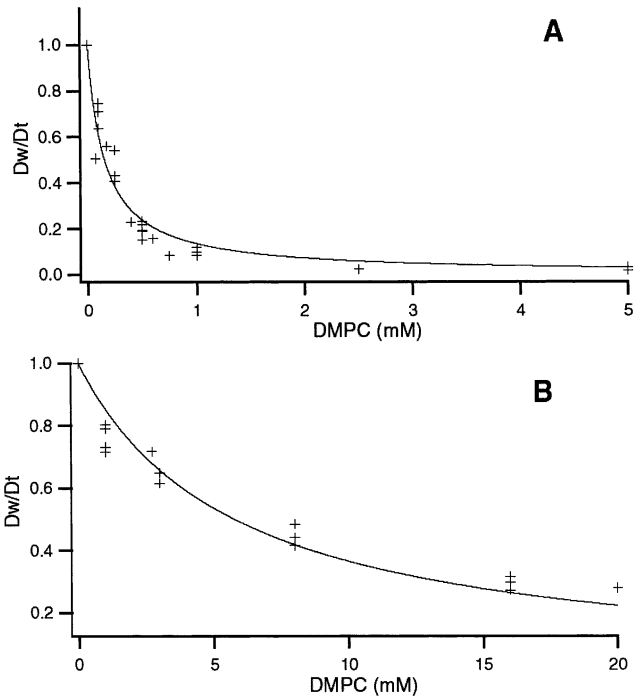

Figure 7. Partitioning of apo-M_E (A) and Fe−M_E (B) into DMPC vesicles. A 16.2 μM concentration of apo-M_E or a 20 μM concentration of Fe−M_E was mixed with varying concentrations of LUVs. Following equilibration, siderophore−vesicle suspensions were ultracentrifuged and the supernatant was assayed for siderophore concentration by HPLC. The ratio of siderophore in solution to the initial concentration (D_W/D_T) is plotted versus the lipid concentration. The solid lines are fits to the experimental data according to eq 8. The partition coefficient for apo-M_E is (6.4 ± 0.5) × 10^3 M^{-1}, and that for Fe−M_E is 174 ± 14 M^{-1}.

inversely proportional to the lipid concentration as shown in Figure 7. Assuming a dilute solution whereby the partition coefficient (K) was expressed as

$$K = D_L/[L]D_W \qquad (7)$$

and the plot was fit to the function

$$D_W/D_T = 1/[K(L) + 1] \qquad D_T = D_W + D_L \qquad (8)$$

where D_L is the amount of siderophore in the lipid phase. The results from two independent sets of experiments each for apo-M_E and Fe−M_E agreed within the experimental error of the measurements. The partition coefficient ($K^*_{\text{apo-}M_E}$) in LUVs for apo-M_E is (6.4 ± 0.5) × 10^3 M^{-1} (see Figure 7A), and that for Fe−M_E is 174 ± 14 M^{-1} (see Figure 7B). Thus, in both SUV and LUV systems, the partition coefficient of apo-M_E was found to be about 50 times larger than that of Fe−M_E.

Partitioning Effects of the Physiological Mixture of Marinobactins As Determined in LUVs. Partition experiments were performed on the suite of marinobactins M_A−M_E (Figure 1) by equilibration of the physiological mixture with LUVs and subsequent ultracentrifugation and quantification of each marinobactin (D_W) by HPLC. A significant difference exists between the HPLC chromatograms of the physiological mixture prior to and following equilibration with DMPC vesicles (Figure 8). For each marinobactin, analysis of the ratio D_W/D_L (averaged value) as a function of vesicle concentration showed a hyperbolic dependence similar to that previously seen for apo-M_E and Fe−M_E (Figure 9). A partition coefficient of (5.8 ± 0.7) × 10^3 M^{-1}

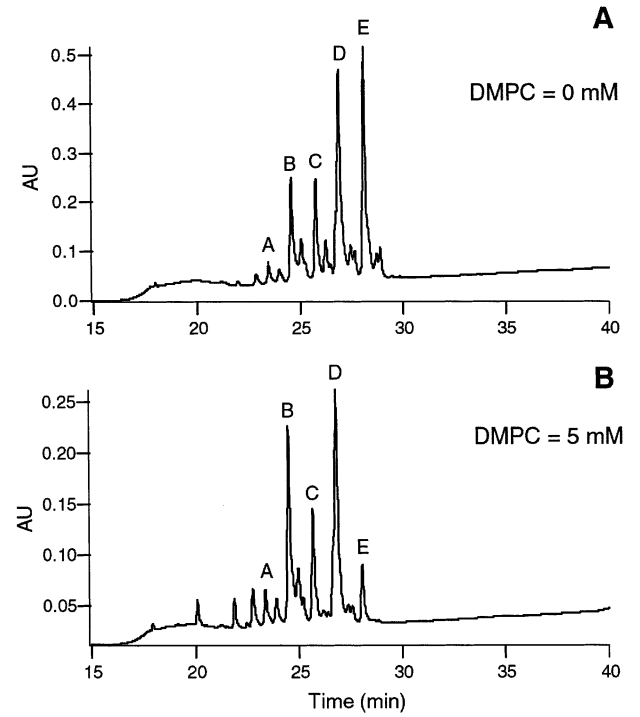

Figure 8. HPLC chromatograms of the physiological mixture prior to (A) and following (B) equilibration with DMPC vesicles (LUVs). The lettering above each peak denotes the marinobactin as shown in Figure 1. Note the difference in scale of the y axis (absorbance units) from (A) to (B).

was determined for apo-M_E, which is in agreement, within experimental error, to that determined with purified apo-M_E

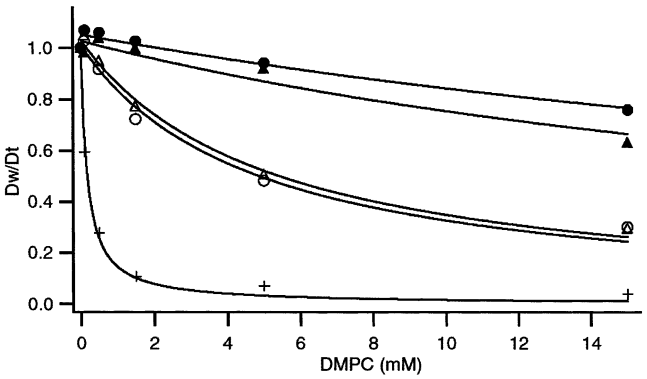

Figure 9. Partitioning of the physiological mixture into DMPC vesicles. The ratio of siderophore in solution to the initial concentration (D_W/D_T), for each marinobactin, is plotted versus the lipid concentration. The solid lines are fits to the experimental data according to eq 8. Partition coefficients and symbols for each siderophore in the mixture are as listed: apo-M_E (+, 5818 ± 694 M^{-1}); apo-M_D (○, 209 ± 28 M^{-1}); apo-M_C (△, 195 ± 21 M^{-1}); apo-M_B (●, 25 ± 4 M^{-1}); apo-M_A (▲, 36 ± 7 M^{-1}).

(Figure 7A). Interestingly, the partition coefficient determined for apo-M_E is 1 order of magnitude larger than that of apo-M_D; the difference between these two siderophores is the addition of one unit of unsaturation in the acyl chain (the ratio of apo-M_{D2} to apo-M_{D1} was roughly 3:1). A similar difference was seen between apo-M_C and apo-M_B, which again differ by one unit of unsaturation. Furthermore, an additional order of magnitude difference is seen when the acyl chain length is reduced by two methylene carbons (apo-M_E to apo-M_C). A significant amount of error is associated with determining partition coefficients for apo-M_B and apo-M_A; however, they do show a general trend toward a lesser degree of partitioning.

Discussion

Comparison of the Membrane Affinities of Apo-M_E and Fe−M_E. The interaction of the marinobactins with phospholipid vesicles is of interest for elucidating the molecular mechanisms involved in iron sequestration mediated by these unusual amphiphilic siderophores. The results show that iron acquisition by apo-M_E follows the scenario depicted in Scheme 1. Both apo-M_E and Fe−M_E display appreciable membrane affinity.[42] However, apo-M_E was found to bind to the lipid phase much more strongly than Fe−M_E. The associative properties of apo-M_E are very similar to those of the lipopeptide surfactin, a detergent-like peptide produced by *Bacillus subtilis*[43,44] (a CMC of 7.5 μM and a partition coefficient of $\sim 5 \times 10^4$ M^{-1}). The results show that, upon formation of the iron(III) complex (Fe−M_E), the partition coefficient of the marinobactin decreased by about 50-fold, although its CMC only increased by 2-fold. For nonionic detergents the free energies of micellization correlate linearly with partitioning, such that a double logarithmic plot of K versus CMC shows a linear relationship corresponding to $K(\mathrm{CMC}) = 1$.[43,45] A similar comparison for apo-M_E and Fe−M_E suggests that apo-M_E roughly agrees with the above linear relationship; however, for Fe−M_E the experimentally determined partition coefficient is significantly lower than would be predicted from the CMC.[17] This difference is curious as one would assume that the hydrophobic effect, driving the process of micellization, would also largely contribute toward the degree of partitioning in vesicles.[46]

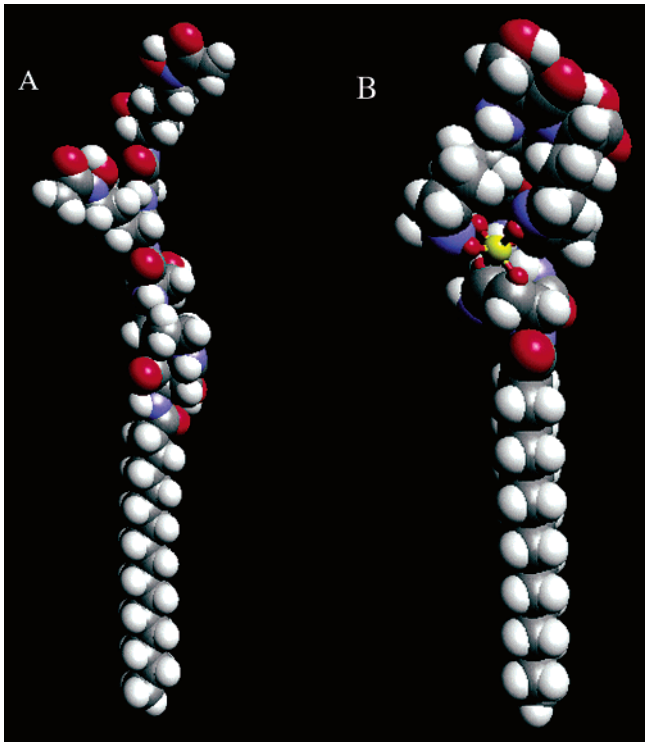

Figure 10. Approximate molecular conformations of (A) apo-M_E and (B) Fe−M_E derived from MM2 methods using Chem3D and Spartan molecular graphics packages. The color code is standard: C, gray; H, white; O, red; N, blue. The iron coordination core is represented by the yellow octahedral structure in (B), in which the small red spheres are the ligating oxygen atoms.

This large decrease in the membrane affinity of Fe−M_E could be related to the significant change in the geometry and conformation of the headgroup that must occur upon binding iron (Figure 10). The extended conformation of apo-M_E shown in Figure 10A has all of the amide bonds in the trans configuration, with a minimum of gauche interactions. However, for all reasonable structures of the iron complex, the two hydroxamate ligands fold to form a tight, six-coordinate octahedral cage around the iron(III) with the α-hydroxy lactam in the nine-membered ring (Figure 10B). As a result of this clam-shell-like fold, the hydrophilic headgroup in Fe−M_E becomes more spherical with all the oxygen and nitrogen atoms distributed around the periphery of the core and directed toward the aqueous environment.

Biological Implications of the Siderophore Membrane Affinity. The partition coefficients for the suite of naturally occurring marinobactins varied over 3 orders of magnitude and showed a strong dependence on the length of the fatty acid chains (Figure 9). An order of magnitude difference is seen between the partitioning of apo-M_E to apo-M_C and apo-M_C to apo-M_A. This difference is as expected since both contain

(42) The membrane partition coefficients of apo-M_E and Fe−M_E are on the order of those of other membrane-active detergents such as octyl glucoside, Triton X-100, and sodium cholate (K ranging from 44 to 3430 M^{-1}); cf. ref 46.
(43) Heerklotz, H.; Seelig, J. *Biophys. J.* **2001**, *81*, 1547−1554.
(44) Bonmatin, J. M.; Genest, M.; Petit, M. C.; Gincel, E.; Simorre, J. P.; Cornet, B.; Gallet, X.; Caille, A.; Labbe, H.; Vovelle, F.; Ptak, M. *Biochimie* **1992**, *74*, 825−836.
(45) Heerklotz, H.; Seelig, J. *Biophys. J.* **2000**, *78*, 2435−2440.
(46) (a) Inoue, T. In *Vesicles*; Rosoff, M., Ed.; Marcel Dekker: New York, 1996; Vol. 62, pp 151−193. (b) Tsao, H. K.; Tseng, W. L. *J. Chem. Phys.* **2001**, *115*, 8125−8132.
(47) Hoyrup, P.; Davidsen, J.; Jorgensen, K. *J. Phys. Chem. B* **2001**, *105*, 2649−2657.

saturated fatty acid tails each differing by two methylene carbons (Figure 1). A similar phenomenon was seen with lysoplipids and saturated fatty acids.[47] Furthermore, we see a greater membrane affinity for the siderophores containing saturated versus unsaturated fatty acid tails owing to the more hydrophilic nature of the unsaturated chain than the homologous saturated chain.[48] These experiments suggest that producing a suite of siderophores would create a concentration gradient extending from the bacterium. In contrast to more traditional soluble siderophores, the marinobactins and other lipophilic siderophores present a novel method to counter apo-siderophore diffusion while releasing the iron−siderophore complex for receptor-mediated uptake. A membrane-bound siderophore could also limit a three-dimensional search in space normally required for interaction with a specific receptor to a two-dimensional search within the membrane.[49]

Summary and Conclusions

The thermodynamics of the membrane partitioning of marinobactin E and its iron(III) complex were studied using both SUVs and LUVs as model membrane systems. Apo-M_E was found to have a strong affinity for lipid membranes, but this association was shown to decrease the rate of iron(III) binding by only a factor of 2. Upon chelating iron(III), the affinity of this siderophore for the membrane decreased 50-fold. This differentiation in membrane affinity could provide unique biological advantages in a receptor-assisted iron acquisition process by countering losses of apo-M_E due to diffusion while making the iron complex Fe−M_E more available.

Acknowledgment. We are grateful to the National Science Foundation and the Department of Energy for funding this research through the Environmental Molecular Science Institute (CEBIC), Grant NSF9810248 (J.T.G. and A.B.). We also acknowledge support from the NIH through Grant GM38130 (A.B.) and the NSF through Grant CHE 9814301 (J.T.G.). Partial support via California Sea Grant NA66RG0447, Project R/MP-76 (A.B.), and Sea Grant Fellowship support (J.S.M.) funded by a grant from the National Sea Grant College Program, National Oceanic and Atmospheric Administration, and the U.S. Department of Commerce are gratefully acknowledged. Fellowship support for G.X. from the Princeton Materials Institute and Johnson & Johnson Co. is gratefully acknowledged. We thank Prof. Margo Haygood (Scripps Institution of Oceanography, University of California, San Diego) for continuing collaboration on iron sequestration by marine bacteria.

Supporting Information Available: Derivations of eqs 2, 3, and 6 (PDF). This material is available free of charge via the Internet at http://pubs.acs.org.

JA026768W

(48) Damas, C.; Vannier, L.; Naejus, R.; Coudert, R. *Colloids Surf.* **1999**, *152*, 183−187.
(49) Epand, R. M. *Biopolymers* **1997**, *43*, 15−24.